Published in final edited form as:
Acta Biomater. 2012 July ; 8(6): 2213–2222. doi:10.1016/j.actbio.2012.03.017.

FGF-1 and proteolytically-mediated cleavage site presentation influence 3D fibroblast invasion in biomimetic PEGDA hydrogels

Sonja Sokic[a] and **Georgia Papavasiliou**[a,*]
[a]Department of Biomedical Engineering, Illinois Institute of Technology, Chicago, IL 60616, USA

Abstract

Controlled scaffold degradation is a critical design criterion for the clinical success of tissue engineered constructs. Here, we exploited a biomimetic poly(ethylene glycol) diacrylate (PEGDA) hydrogel system immobilized with tethered YRGDS as the cell adhesion ligand and with either single (SSite) or multiple (MSite) collagenase-sensitive domains between crosslinks, to systematically study the effect of proteolytic cleavage site presentation on hydrogel degradation rate and 3D fibroblast invasion *in vitro*. Through the incorporation of multiple collagenase-sensitive domains between crosslinks, hydrogel degradation rate was controlled and enhanced independent of alterations in compressive modulus. As compared to SSite hydrogels, MSite hydrogels resulted in increased 3D fibroblast invasion *in vitro* which occurred over a wider range of compressive modulus. Furthermore, encapsulated soluble acidic fibroblast growth factor (FGF-1), a potent mitogen during processes such as vascularization and wound healing, was incorporated into SSite and MSite PEGDA scaffolds to determine its *in vitro* potential on fibroblast cell invasion. Hydrogels containing soluble FGF-1 significantly enhanced 3D fibroblast invasion in a dose-dependent manner within the different types of PEG matrices investigated over a period of 15 days. The methodology presented provides flexibility in designing PEG scaffolds with desired mechanical properties, but with increased susceptibility to proteolytically-mediated degradation. These results indicate that effective tuning of initial matrix stiffness and hydrogel degradation kinetics plays a critical role in effectively designing PEG scaffolds that promote controlled 3D cellular behavior and in situ tissue regeneration.

Keywords

Biodegradation; Biomimetic Material; Free-radical; Cross-linking; Fibroblast growth factor; fibroblasts

1. Introduction

Tissue engineering and regenerative medicine focuses on the design and development of scaffolds with mechanical and biochemical cues that direct cell behavior aimed towards the *in vitro* construction and the *in vivo* induction of tissue. While scaffolding materials from naturally derived sources possess the structural complexity and functional capacity of a particular tissue of interest, these biomaterials are associated with immunogenicity, batch-to-batch variability, and lack the ability to alter mechanical and degradative properties independent of variations in biochemical composition. As an alternative approach, synthetic

*Corresponding author. Tel.: + 1 312 567 5959, fax: + 1 312 567 5770, papavasiliou@iit.edu (G. Papavasiliou).

polymeric matrices have been extensively investigated as scaffolds in tissue engineering due to their ability to systematically incorporate biofunctional signals of the native extracellular matrix (ECM) and fine-tune mechanical properties in a highly reproducible manner, thus allowing for controlled study of cell-substrate interactions.

Among the classes of synthetic scaffolds, crosslinked poly(ethylene glycol) (PEG) hydrogels have been extensively used in tissue engineering due to their hydrophilicity, biocompatibility, and ability to be biochemically modified. Various approaches have been used to fabricate PEG hydrogels with covalently incorporated ECM signals such as free-radical photopolymerization [1–6], step-growth polymerization such as Michael-type addition [7], combinations of free radical and step-growth chemistries (mixed mode polymerization) [8, 9], *Click* chemistry [10], and native chemical ligation [11]. To this end, studies have shown that the incorporation of soluble and immobilized biofunctional cues within these scaffolds as well as their mechanical properties [12] dictate cell behavior *in vitro* [1, 13–16] and *in vivo* [13, 16, 17]. To render these scaffolds susceptible to 3D cell adhesion, proteolytic degradation, proliferation, migration and matrix deposition, cell adhesion ligands such as RGD as well as cleavable peptide domains sensitive to cell-mediated proteolysis have been covalently immobilized into PEG hydrogels [12, 15, 16, 18]. Studies have also shown that growth factor immobilization enhances adhesion and migration [15, 16], and that the presence of both soluble and immobilized growth factors results in enhanced cell-mediated proteolysis [15].

Controlled scaffold degradation is a critical design criterion for successful tissue regeneration. This requires that hydrogel degradation be matched with tissue regeneration at the defect site [19]. Hydrogel degradation rates that either exceed or significantly lag the rates of tissue regeneration will impede cell growth, invasion, and migration within the scaffold and consequently prevent neo tissue formation. While PEG hydrogels with pre-engineered degradation rates have been fabricated with hydrolytically degradable segments for regenerative medicine applications [20, 21], these systems lack the ability to modify degradation rates post-scaffold fabrication [10]. Therefore, proteolytic degradation mechanisms of the native ECM that are responsive to cell-secreted enzymes have been engineered into PEG hydrogels in the form of crosslinkable peptide domains sensitive to cell-mediated proteolysis [22]. Although PEG-based materials with crosslinked peptide domains cleavable by cell- secreted proteases have shown promise for *in vivo* tissue engineering repair applications, the remodeling rate of these hydrogels may be too slow, limiting cellular invasion. To address this issue, recent strategies have focused on enhancing the proteolytic degradation of PEG hydrogels by targeting peptide substrates with increased catalytic activity [18] or by increasing the incorporation of proteolytically degradable crosslinks within the hydrogel network [23]. While most PEG studies to date have investigated the effects of specific immobilized ECM signals and hydrogel mechanical properties on 3D cell behavior, the tuning of hydrogel degradation rate independent of alterations in the initial mechanical properties (i.e., prior to gel degradation) to our knowledge, has not been previously investigated. The aim of this study was to control hydrogel mechanical properties and proteolytically-mediated gel degradation within synthetic photopolymerized PEG diacrylate (PEGDA) hydrogel scaffolds and to investigate these effects on 3D fibroblast cell invasion *in vitro*. Through alterations in the molecular weight of the protease-sensitive PEGDA crosslinking macromer as well as variations in the number of collagenase-sensitive peptide domains between the terminal acrylate groups of the PEGDA crosslinking agent, we are able to enhance fibroblast invasion by uncoupling alterations in hydrogel modulus from proteolytically mediated hydrogel degradation. PEGDA hydrogels were rendered degradable by crosslinking PEGDA macromers containing either single (SSite) or multiple (MSite) collagenase-sensitive peptide domains between acrylate groups in the presence of cell adhesion ligand macromers of acrylate-

PEG_{3400}-YRGDS. In addition, acidic fibroblast growth factor (FGF-1) was encapsulated in soluble form in the presence of cells within these hydrogels to investigate its effect on 3D fibroblast invasion. FGF-1 is the broadest acting member of the FGF family as it is known to bind to all FGF-receptor subtypes with high affinity [24] and has been shown to be a potent mitogenic and chemotactic agent of numerous cell types including dermal fibroblasts, vascular endothelial cells, and epidermal keratinocytes [25]. Its wide range of biological activity gives rise to many potential clinical applications such as vascularization and enhanced wound healing within tissue engineered constructs [26]. The effect of FGF-1 on 3D cell invasion within PEG hydrogels to our knowledge has not been previously explored. In this paper, we quantify 3D fibroblast invasion in SSite and MSite photopolymerized PEGDA hydrogels *in vitro* over a time course of 15 days as a function of hydrogel mechanical properties, degradation rate, and soluble FGF-1 concentration.

2. Materials and Methods

2.1. Cell Culture

NIH 3T3 fibroblasts were cultured in Dulbecco's modified Eagle's medium (DMEM) supplemented with 10% fetal bovine serum (FBS) and 1% Penicillin (5000 I.U./mL)-Streptomycin (5 mg/mL) (Pen-strep). Cells were cultured in an incubator at 37 °C and 5% CO_2. Medium was replenished every 2 days. DMEM, FBS, and Pen-Strep were obtained from Fisher Scientific (Hanover Park, IL).

2.2. Synthesis of PEG-peptide Conjugates

Hydrogels were rendered degradable to cell-mediated proteolysis through the covalent incorporation of the collagenase-sensitive peptide sequence, GGL↓GPAGGK (↓ indicates cleavage point by collagenase between the leucine and glycine residues) (American Peptide, Sunnyvale, CA). PEGDA macromers were conjugated using SVA chemistry to incorporate either single (SSite) or multiple (MSite) collagenase-sensitive domains between acrylate groups as shown in Scheme 1. SSite degradable macromers were synthesized by dissolving the peptide in 50 mM $NaHCO_3$ (pH 8.0) and reacting with Acrylate-PEG-succinimidyl-valerate (acrylate-PEG-SVA, MW =3400 Da and 8000 Da, Laysan Bio, Arab, AL) in a 2:1 PEG:peptide molar ratio. The resulting products, acrylate-PEG-peptide-PEG-acrylate, with theoretical molecular weights of 7,512.8 Da and 16,712.8 Da, were dialyzed, lyophilized, and stored frozen at −20 °C. MSite degradable PEGDA macromer was synthesized via modification of a previously published protocol [27]. In a stepwise manner, the peptide was first reacted with acrylate-PEG-SVA (MW 3400 Da) in equal molar ratios. The product was then dialyzed and lyophilized to remove undesired products. This acrylate-PEG-peptide was further reacted with SVA-PEG-SVA (MW 3400 Da) (Laysan Bio, Arab, AL) and additional peptide, dialyzed and lyophilized. The reaction step was repeated to add additional PEG-peptide. In the final step, the previous product was reacted with acrylate-PEG-SVA (MW 3400 Da) to form the MSite degradable PEGDA macromer. The final product acrylate-$(PEG\text{-}peptide)_3$-PEG-acrylate (theoretical MW ~15,238.4 Da) was dialyzed, lyophilized and stored at −20 °C. In a similar manner, the cell adhesive ligand YRGDS (American Peptide) was conjugated to PEG by reacting acrylate-PEG-SVA (MW 3400 Da) with YRGDS in a 1:1 PEG:peptide molar ratio. The product acrylate-PEG_{3400}-YRGDS was dialyzed to remove unwanted products and lyophilized. PEGDA macromers were analyzed using Gel Permeation Chromatography (GPC) equipped with refractive index, viscometery, and light scattering detection (Viscotek Triple Detector Array and GPCmax, Malvern Instruments Ltd, Worcestershire, UK). GPC analysis of macromer samples was performed by PolyAnalytik Inc. (London, Ontario).

2.3. PEGDA Hydrogel Photopolymerization

Hydrogels were formed using 100 μL of a PEG precursor solution (3 and 5% w/v) consisting of 37 mM N-vinylpyrrolidone (NVP), 225 mM triethanolamine (TEA) and 0.05 mM of the photosensitive dye, eosin Y, in phosphate buffered saline (PBS) adjusted to pH 7.4 and photopolymerized by exposure to visible light (λ =514 nm) using an Argon Ion Laser (Coherent Inc. Santa Clara, CA) at a laser flux of 100 mW/cm^2. All chemicals were purchased from Sigma (St. Louis, MO).

2.4. Quantification of Hydrogel Swelling Properties

PEGDA hydrogels were polymerized and allowed to swell for 24 hours. The mass of the swollen hydrogel (M_s) was obtained by removal of the excess fluid. The mass of the dried hydrogel (M_d) was obtained by drying in a vacuum oven for 3 days at 50 ºC. The swelling ratio (Q) was then calculated using the equation: $Q= M_s/M_d$.

2.5. Quantification of Hydrogel Mechanical Properties

The mechanical properties of PEGDA hydrogels were quantified using compression experiments. Hydrogels were photopolymerized and allowed to reach equilibrium swelling before being loaded onto a TA RSA3 mechanical tester (TA Instruments, New Castle, DE) controlled by TA Orchestrator software. Samples were compressed at a constant strain rate of 0.5 mm/min [28] using a 10N load cell to obtain a stress versus strain curve. This strain rate ensured that the compressive modulus was calculated from the slope of the linear region of the stress strain curve at less than 10% (r^2>98%) as previously reported [29, 30].

2.6. Quantification of Hydrogel Degradation Kinetics

Hydrogels were allowed to swell for 24 hrs in PBS with 1mM $CaCl_2$ at 37 °C. Each hydrogel was incubated at 37 °C with 1 mL of 0.1 mg/mL collagenase from Clostridium hystolyticum (Sigma, St. Louis, MO) in PBS with 1mM $CaCl_2$. The change in wet weight of the hydrogels ;as measured over time.

2.7. Cell Encapsulation and Quantification of Fibroblast Invasion in Collagenase-Sensitive PEGDA Hydrogels

For fibroblast invasion studies, hydrogel precursor was prepared in DMEM (pH 7.4) with acrylate-PEG_{3400}-YRGDS (15mg/mL), varying concentration of 0, 50, and 100 ng/mL soluble FGF-1 (R&D Systems, Minneapolis, MN) and 5 U/mL heparin (APP Pharmaceuticals, Schaumburg, IL). Fibroblast spheroids (10,000 cells/spheroid) were formed with regular maintenance media containing 0.24 % (w/v) carboxymethylcellulose (Sigma). Cells were seeded into non-adherent round-bottom 96 well plates and incubated at 37 ºC, 5% CO_2 for 24 hrs. The cell spheroids were encapsulated in the hydrogels by placing the spheroid in the core of the precursor (50 μL volume) prior to polymerization. The hydrogels were allowed to swell for 24 hours in DMEM at 37 °C and 5% CO_2. Media was changed after the first 24 hours, then every 2 days. To quantify cell invasion into the surrounding collagenase-sensitive hydrogel matrix, aggregates were imaged every 2 days with an Axiovert 200 inverted microscope equipped with a 12-bit monochromatic AxioCam MR5 digital camera (Carl Zeiss, Gottingen, Germany) using a 5X objective. Fibroblast invasion was quantified from the obtained images using AxioVision 4.2 Image Analysis Software by subtracting the projected area of the encapsulated spheroid on day 1 from days 1 through 15.

2.8. Cell Viability and Confocal Microscopy

The viability of fibroblast aggregates within PEG hydrogels was evaluated qualitatively using a LIVE/DEAD staining kit (Invitrogen, Eugene, OR) 24 hrs and 15 days post

encapsulation. Briefly, hydrogels were rinsed with PBS and incubated with LIVE/DEAD staining reagents calcein AM (green fluorescent dye which stains live cells) and ethidium homodimer-1 (red fluorescent dye which stains dead cells) for 1 hour following the manufacturer's protocol. Stained aggregates were imaged with confocal microscopy using a Pascal Laser scanning microscope (LSM) system from Carl Zeiss MicroImaging, Inc. (Thornwood, NY) at 20 μm sections projected into single plane images.

2.9. Statistics

All data are presented as mean ± standard deviation (S.D.). Statistical analyses were performed with analysis of variance (ANOVA) followed by Tukey's HSD test for multiple comparisons (SigmaStat 3.5). Probability (p) values <0.05 were considered statistically significant.

3. Results

3.1. Characterization of the Physical and Mechanical Properties of Collagenase-Sensitive PEGDA Hydrogels

Alterations in hydrogel compressive modulus and swelling ratio were obtained through slight alterations in the polymerization conditions. Figure 1 displays the swelling ratio of the different PEG hydrogel types as a function of the compressive modulus. In general, an increase in the compressive modulus resulted in a decrease in the swelling ratio. At a constant hydrogel swelling ratio of ~46 among all PEG types, the compressive modulus varied from 280 ± 38 Pa to 495 ± 98 Pa. However, a decrease in the hydrogel swelling ratio to ~43 resulted in a statistically significant increase in the compressive modulus in all PEG types with compressive modulus values ranging from 1137 ± 54 Pa to 1628 ± 87 Pa. Additionally, increases in the MW of the PEGDA macromer from 8kDa to 16kDa resulted in a statistically significant decrease in the compressive modulus.

3.2. Analysis of Degradation Kinetics of Collagenase-Sensitive PEGDA Hydrogels

The degradation rates of PEG scaffolds formed from SSite and MSite PEGDA macromers were quantified by monitoring changes in the wet weight of the hydrogels in the presence of collagenase enzyme over time. Figure 2 shows the gel degradation profiles as a function of the various PEGDA macromer types used to crosslink the hydrogels and the corresponding resultant compressive modulus. The data in Figure 2 are also representative of cases that resulted in a range of matrix properties that promoted 3D cell invasion as detailed below. In general, the time for complete hydrogel degradation increased with increasing hydrogel compressive modulus which correlates to increases in crosslink density, decreases in swelling and hence diffusion of the collagenase enzyme though the gel. Furthermore, hydrogels within the SSite group formed from 16 kDa and 8 kDa PEGDA macromers that exhibited lower compressive modulus values of 280 ± 38 Pa and 405 ± 87 Pa, respectively, had statistically different degradation profiles, with complete hydrogel degradation times of 1.5 and 2 hours. At higher compressive modulus values of 1191 ± 67 Pa and 1628 ± 87 Pa for SSite 16kDa versus 8kDa groups, respectively, more pronounced differences in the hydrogel degradation profiles were observed corresponding to statistically significant differences in degradation times of 3.5 and 5 hours, respectively.

Interestingly, comparisons of MSite (16kDa) versus SSite (8kDa) hydrogel groups that possessed similar values in compressive modulus (495 ± 98 Pa vs. 405 ± 87 Pa, respectively) demonstrated that MSite gels exhibited statistical significant increases in degradation. The increased degradation rate observed in hydrogels possessing a similar modulus but a larger number of collagenase-sensitive domains between crosslinks was again observed when comparing SSite 16kDa versus MSite 16kDa PEGDA hydrogels.

Specifically, MSite gels with a compressive modulus of 1137 ± 54 Pa achieved complete degradation within 3 hours which was found to be a statistically lower degradation time than that of SSite hydrogels with a compressive modulus of 1191 ± 67 Pa and a corresponding degradation time of 3.5 hours. In addition, 3D cell invasion was only found to occur in the MSite and not in the SSite hydrogels even though these two types of matrices exhibited a similar compressive modulus (~ 1100 Pa) as described below.

3.3. Effect of FGF-1 Concentration and Matrix Properties on 3D Fibroblast Invasion

Acidic fibroblast growth factor (FGF-1) has been shown to be a potent mitogenic and chemotactic agent for fibroblasts and endothelial cells thus playing an important role in processes such as neovascularization and wound healing [24, 26]. The rate of fibroblast invasion within collagenase-sensitive PEG hydrogels (SSite and MSite) was therefore evaluated as a function of soluble FGF-1 concentration in the presence of heparin. Heparin is known to facilitate the binding of FGF-1 to the transmembrane FGF receptor and was therefore encapsulated with FGF-1 in the presence of cells for *in vitro* studies [31]. Briefly, fibroblast cell clusters were encapsulated into hydrogels that contained varying concentrations of soluble FGF-1 and the rate of fibroblast invasion was monitored over time. Fibroblast aggregates invaded the surrounding matrix within 3–5 days and formed thin sprouts, which over time established more interconnections and grew radially outward (Fig. 3B). As shown in Figure 3A, the addition of soluble FGF-1 resulted in a dose-dependent increase in cell invasion throughout the time course. Statistically significant increases in fibroblast invasion occurred between the no FGF-1 control group as compared to both the 50 and 100 ng/mL FGF-1 groups over the time course investigated. No statistical significant differences were found to occur between the 50 and 100 ng/mL FGF-1 groups (Fig.3A). Therefore, the effect of FGF-1 on cell invasion was investigated with FGF-1 concentrations of 0 and 100 ng/mL FGF-1 in all subsequent studies. As shown in Figure 4, regardless of the PEG type investigated and the resultant mechanical properties, the addition of FGF-1 resulted in a statistical significant increase in fibroblast invasion.

In an effort to reduce the cellular response to exogenous factors in growth factor studies, experiments may be carried out at low serum conditions. To assess the effect of serum concentration on fibroblast invasion and FGF-1 concentration simultaneously, three different serum concentrations were investigated (1%, 5%, and 10%) with 0 and 100 ng/mL FGF-1 and 5U/mL heparin in MSite gels. Fibroblast invasion resulted in a statistically significant increase in response to either increases in serum or FGF-1 concentration (Fig. 5). On day 15, fibroblast invasion for 1%, 5%, and 10% serum concentrations without soluble FGF-1 was 0.12 ± 0.08 mm^2, 1.07 ± 0.13 mm^2, and 1.39 ± 0.15 mm^2, respectively. The addition of 100 ng/mL FGF-1 and 5U/mL heparin increased the projected area of invading fibroblasts cultured with 1%, 5%, and 10% serum concentration to 0.22 ± 0.07 mm^2, 1.55 ± 0.66 mm^2, and 1.89 ± 0.35 mm^2, respectively. Over the time course of invasion, fibroblast invasion into the surrounding matrix was significantly lower at low serum concentrations (1%) as compared to 5% and 10% serum concentrations. In addition, at low serum concentration (1%), fibroblasts invaded the matrix primarily as individual cells while at higher serum concentrations, fibroblast sprouts appeared to form more interconnections while invading the hydrogel matrix (Fig. 6). Since invasion increased in response to both serum concentration and FGF-1, all subsequent studies were completed in the full serum condition.

Fibroblast invasion was also quantified as a function of hydrogel compressive modulus and cleavage site presentation in the presence and absence of encapsulated soluble FGF-1 (Fig. 7). Within the no FGF-1 group, hydrogels formed with SSite PEGDA macromers of variable MW (8kDa and 16kDa) resulted in a statistically significant increase in fibroblast invasion with decreasing compressive modulus (Fig. 7A–C). The differences in invasion were

observable by day 5 (Fig. 7A) and day 9 (Fig. 7B) but were more pronounced by day 15 (Fig. 7C). On day 15, fibroblast invasion was 0.45 ± 0.08 mm² and 1.87 ± 0.47 mm², with corresponding compressive modulus values of 405 ± 87 Pa and 280 ± 38 Pa, within hydrogels formed with SSite 8kDa versus SSite 16kDa macromers, respectively. Furthermore, the encapsulation of 100 ng/mL FGF-1 within these matrices increased the invasion to 2.11 ± 0.67 mm² (SSite 8kDa) and 3.28 ± 0.98 mm² (SSite 16kDa). Furthermore, more substantial increases in invasion for hydrogels formed in the presence of entrapped soluble FGF-1 were observed in the lower molecular weight SSite 8kDa hydrogel group as compared to the 16kDa SSite hydrogel group. In SSite 8kDa gels, the addition of 100 ng/mL FGF-1 increased fibroblast invasion 4.7 fold compared to a 1.75 fold increase in SSite 16kDa gels (Fig. 7C), although these were not found to be statistically significant. This observed relative increase in cell invasion within SSite 8 kDa hydrogels may be attributed to the decrease in diffusion of encapsulated FGF-1 associated with increased stiffness and decreased swelling ratio as compared to higher molecular weight SSite 16kDa hydrogels. Fibroblasts failed to invade hydrogels crosslinked with SSite PEGDA macromers with molecular weights of 8kDa and 16kDa and a corresponding compressive modulus of 1628 ± 87 Pa and 1191 ± 67 Pa.

Interestingly, hydrogels crosslinked with MSite PEGDA (MW = 16kDa) macromers resulted in fibroblast invasion over a wider range of mechanical properties (495 ± 98 Pa and 1137 ± 54 Pa) with small differences in the invasion profile observed in this range of modulus. Additionally, comparisons of hydrogel groups with similar compressive modulus, specifically MSite 16kDa (compressive modulus = 495 ± 98 Pa) versus SSite 8kDa (compressive modulus 405 ± 87 Pa) hydrogels demonstrated small differences in fibroblast invasion on day 5 (Fig. 7A) with statistically significant increases in invasion observed by days 9 (Fig. 7B and 8) and 15 (Fig. 7C). Fibroblasts also invaded stiffer hydrogel matrices formed from MSite 16kDa PEGDA hydrogels (compressive modulus =1137 ± 54 Pa) while no invasion occurred within the SSite 16kDa hydrogels of similar compressive modulus (1191 ± 54 Pa). LIVE/DEAD staining showed that fibroblast aggregates remained viable 15 days post encapsulation regardless if the hydrogels supported invasion after 15 days (Fig. 9). These results suggest that this biomimetic hydrogel system supports the encapsulation of fibroblasts with minimal compromise of cell viability. Furthermore, increases in the presentation and concentration of collagenase-sensitive domains within these hydrogels result in enhanced cell-mediated proteolysis, degradation, and fibroblast invasion.

4. Discussion

In this study, PEGDA hydrogels immobilized with SSite and MSite collagenase-sensitive domains between crosslinks, with pendant YRGDS, and entrapped with soluble FGF-1 were formed by free-radical photopolymerization in the presence of visible light and were investigated as matrices for the support of 3D fibroblast invasion *in vitro*. We and others have shown that alterations in polymerization conditions affect hydrogel mechanical properties as well as the presentation of biochemical signals within hydrogels, which in turn dictate cell behavior [1, 3–6, 13, 32]. In this study, the physical and mechanical properties of collagenase-sensitive PEGDA hydrogels were altered independent of alterations in proteolytically-mediated degradation that allowed for the quantification of the effects of gel degradation rate and compressive modulus on fibroblast invasion. Furthermore, increases in proteolytic cleavage site presentation achieved in MSite hydrogels resulted in cell invasion over a wider range of modulus values (495 ± 98 Pa - 1137 ± 54 Pa) as compared to invasion in SSite hydrogels that occurred over a modulus range of 280 ± 38 Pa to 405 ± 87 Pa. Previous studies using two-photon laser scanning lithography for guided 3D fibroblast cell migration within collagenase-sensitive PEGDA hydrogel micropatterns have utilized multisite PEGDA macromers by employing alternate reaction protocols for the synthesis of

degradable peptides with heterobifunctional acrylate-PEG-N-hydroxysuccinimide active esters to those presented in our study [6]. However, these studies did not investigate the effects of tuning gel properties on cell behavior. In an effort to increase proteolytic sensitivity of PEGDA hydrogels, a recent study used a step-growth polymerization approach to synthesize matrix-metalloproteinase -(MMP-) sensitive PEGDA macromer conjugates by reacting PEGDA with bis-cysteine MMP-sensitive peptides via Michael-type addition to form high molecular weight (~500kDa) biodegradable photoactive PEGDA macromers of the form acrylate-PEG-$(\text{peptide-PEG})_m$-acrylate [23]. These degradable PEGDA macromer conjugates were crosslinked using UV free-radical photopolymerization to form hydrogels that promoted sprout formation of endothelial cells from embedded embryonic chick aortic arches. However, invasion was not correlated with PEG matrix properties.

In the present study, hydrogel degradation kinetics were investigated both independently and as a function of the physical and mechanical properties of collagenase-sensitive PEGDA hydrogels by changing the MW of the collagenase-sensitive PEGDA macromer as well as the number of cleavage sites between the terminal acrylate groups of PEGDA to yield SSite as well as MSite PEGDA macromers which upon photopolymerization result in alterations in cleavage site incorporation (Scheme 1). To our knowledge, the ability to isolate proteolytically mediated hydrogel degradation from the mechanical properties and quantify the effects of these properties on *in vitro* 3D cell behavior within photopolymerized PEGDA scaffolds has not been previously explored. Recent studies using UV free-radical photopolymerization investigated the effects of mechanical properties and degradation of PEGDA hydrogels immobilized with MMP-sensitive domains and RGD cell adhesion sequences, which served as provisional matrices for vascularization. In this study, however, hydrogels were fabricated with different weight percentages of the MMP-sensitive PEGDA macromer which resulted in simultaneous alterations in hydrogel degradation rate and compressive modulus (~30 kPa −110 kPa) [13]. Specifically, increases in the degradable PEGDA precursor content resulted in increased hydrogel stiffness and degradation time in collagenase solution as the more crosslinked networks took longer to degrade. These hydrogels resulted in the formation of tubule-like structures from endothelial and smooth muscle cell co-cultures after 6 days *in vitro*. However, this was only found to occur at an intermediate stiffness of ~ 60 kPa, which was achieved using an MMP-sensitive PEGDA precursor content of 10 weight percent % to crosslink the scaffolds. At slightly lower PEG macromer precursor content, tubule interconnections regressed as the gels rapidly degraded within 6 days in culture, while slight increases in PEGDA precursor content above 10% resulted in stiffer matrices that prevented cell migration through the highly crosslinked PEG matrix. Although we investigated cell invasion of a different cell type within hydrogels immobilized with a collagenase-sensitive peptide sequence, our data in Figures 7A–C indicate that cell invasion occurs over a range of compressive modulus that is approximately two orders of magnitude less than that reported in this previously published study, but is in agreement with 3D cell proliferation and spreading within MMP-sensitive PEG hydrogels formed via Michael-type addition [12].

Our data also indicate that hydrogels that exhibit a similar compressive modulus, but increased presentation of collagenase-sensitive domains between crosslinks, display enhanced degradation in the presence of collagenase enzyme solution (Fig. 2) and increased cellular invasion *in vitro* over time (Fig. 7). This was further confirmed by the fact that cellular invasion was completely impeded within SSite (MW ~16kDa) hydrogels while cells invaded MSite hydrogels to a substantial degree although both matrices exhibited a similar compressive modulus of approximately 1100 Pa (Fig. 7 and 8). The modulus values obtained in this study may be suitable for the replacement of soft tissues [33, 34], however, increases in the proteolytic cleavage site presentation within PEG hydrogels extends the

stiffness range over which cells can invade these matrices potentially allowing for the regeneration of stiffer tissues such as articular cartilage or skin [35].

Alternative strategies for enhancing proteolytically-mediated hydrogel degradation independent of the mechanical properties of the matrix have relied on the use of protease PEG-peptide substrates with increased enzymatic sensitivity and specificity [18]. PEG hydrogels engineered with a library of peptide substrates that possessed higher catalytic activity and substrate cleavage by MMP-1 and MMP-2 led to enhanced degradation in the presence of these enzymes, in increased cell spreading and proliferation of fibroblasts *in vitro*, and enhanced invasion from gel implanted aortic ring segments. Future studies using our approach may look at incorporating peptide substrates with increased specificity and catalytic activity for promoting enhanced tissue regeneration *in vivo*.

The addition of growth factors in soluble and/or immobilized form within PEG matrices has also been shown to play an important role in required tissue regeneration processes such as vascularization and wound healing. Specifically, PEG matrices immobilized with vascular endothelial growth factor (VEGF) and the cell adhesion ligand RGD and entrapped with transforming growth factor β (TGF-β) have resulted in the conversion of inactive MMP-2 cell-secreted proenzymes into activated form leading to enhanced hydrogel degradation by endothelial cells [15]. In the present study, we explored the potential of physically entrapped acidic fibroblast growth factor (FGF-1) in the presence of heparin towards enhancing fibroblast invasion within collagenase-sensitive PEGDA hydrogels due to its important role in vascularization [24] and matrix remodeling [26]. Our data indicate that a dose-dependent increase in fibroblast invasion in the presence of FGF-1 was found to occur within hydrogels throughout the time course in culture (Fig. 3A). In addition, regardless of the PEG type investigated as well as the resultant gel mechanical properties, the addition of FGF-1 resulted in enhanced fibroblast invasion (Fig. 4 and 7). Future studies will explore soluble FGF-1 release kinetics from PEG hydrogel matrices as well as the effects of soluble versus immobilized FGF-1 in PEGDA matrices on 3D cellular response within these hydrogels.

5. Conclusions

This work presents a detailed investigation of the effects of mechanical, physical, and proteolytically mediated hydrogel degradation on 3D cell invasion within synthetic PEGDA hydrogel scaffolds. Through the alterations in the molecular weight of the crosslinking macromer and variations in the number of collagenase-sensitive domains, the compressive modulus of these biomaterials was controlled independent of proteolytic degradation. Our data indicate that increasing the incorporation of proteolytically-sensitive domains in PEG hydrogel networks through the use of MSite PEGDA macromers at a fixed modulus leads to enhanced degradation and 3D fibroblast invasion over a period of 15 days in culture. Additionally, cells are able to invade MSite hydrogels over a wider range of mechanical properties as compared to SSite hydrogels (Fig. 7 and 8). The addition of soluble FGF-1 within these scaffolds results in further enhancement of fibroblast invasion in a dose-dependent fashion. These studies provide significant insight on the scaffold design criteria leading to enhanced degradation and cell-induced matrix remodeling *in vivo*.

Acknowledgments

We thank Joel Collier for synthesis of the degradable peptides used in our initial studies and Dr. Howard Greisler for donating FGF-1. We would also like to acknowledge Professor David Venerus and Jef Larson for assistance with the compression studies and Bonnie Au for helping with the analysis of aggregate invasion. This work was supported by Award Number R21HL094916 from the National Heart, Lung, and Blood Institute and the Illinois Institute of Technology Educational Research Initiative Fund.

References

1. Leslie-Barbick JE, Moon James JJ, WJL. Covalently-Immobilized Vascular Endothelial Growth Factor Promotes Endothelial Cell Tubulogenesis in Poly(ethylene glycol) Diacrylate Hydrogels. Journal of Biomaterials Science, Polymer Edition. 2009; 20(12):1763–1779. [PubMed: 19723440]
2. Benoit DS, AKS. The effect on osteoblast function of colocalized RGD and PHSRN epitopes on PEG surfaces. Biomaterials. 2005; 26(25):5209–5220. [PubMed: 15792548]
3. Hern DL, HJA. Incorporation of adhesion peptides into nonadhesive hydrogels useful for tissue resurfacing. Journal of Biomedical Materilas Research. 1998; 39(2):266–276.
4. Peyton SR, et al. The use of poly(ethylene glycol) hydrogels to investigate the impact of ECM chemistry and mechanics on smooth muscle cells. Biomaterials. 2006; 27(28):4881–4893. [PubMed: 16762407]
5. Elbert DL, HJA. Conjugate addition reactions combined with free-radical cross-linking for the design of materials for tissue engineering. Biomacromolecules. 2001; 2(2):430–441. [PubMed: 11749203]
6. Moon JJ, et al. Micropatterning of Poly(Ethylene Glycol) Diacrylate Hydrogels with Biomolecules to Regulate and Guide Endothelial Morphogenesis. Tissue Engineering Part A. 2009; 15(3):579–585. [PubMed: 18803481]
7. Metters A, HJ. Network formation and degradation behavior of hydrogels formed by Michael-type addition reactions. Biomacromolecules. 2005; 6(1):209–301.
8. Rydholma AE, Bowman CN, AKS. Degradable thiol-acrylate photopolymers: polymerization and degradation behavior of an in situ forming biomaterial. Biomaterials. 2005; 26(22):4495–4056. [PubMed: 15722118]
9. Salinas CN, AKS. Mixed Mode Thiol-Acrylate Photopolymerizations for the Synthesis of PEG-Peptide Hydrogels. Macromolecules. 2008; 41(16):6019–6026.
10. Lin C, AKS. PEG Hydrogels for the Controlled Release of Biomolecules in Regenerative Medicine. Pharmaceutical Research. 2009; 26(3):631–643. [PubMed: 19089601]
11. Hu BH, Su J, MPB. Hydrogels Cross-Linked by Native Chemical Ligation. Biomacromolecules. 2009; 10(8):2194–2200. [PubMed: 19601644]
12. Bott K, et al. The effect of matrix characteristics on fibroblast proliferation in 3D gels. Biomaterials. 2010; 31(32):8454–8464. [PubMed: 20684983]
13. Moon JJ, et al. Biomimetic hydrogels with pro-angiogenic properties. Biomaterials. 2010; 31(14): 3840–3847. [PubMed: 20185173]
14. Saik JE, et al. Covalently immobilized platelet-derived growth factor-BB promotes antiogenesis in biomirnetic poly(ethylene glycol) hydrogels. Acta Biomaterialia. 2011; 7(1):133–143. [PubMed: 20801242]
15. Seliktar D, et al. MMP-2 sensitive, VEGF-bearing bioactive hydrogels for promotion of vascular healing. Journal of Biomedical Materials Research Part A. 2004; 68A(4):704–716. [PubMed: 14986325]
16. Zisch AH, et al. Cell-demanded release of VEGF from synthetic, biointeractive cell-ingrowth matrices for vascularized tissue growth. FASEB Journal. 2003; 17(13):2260–2262. [PubMed: 14563693]
17. Phelps EA, et al. Bioartificial matrices for therapeutic vascularization. PNAS. 2010; 107(8):3323–3328. [PubMed: 20080569]
18. Patterson J, HJA. Enhanced proteolytic degradation of molecularly engineered PEG hydrogels in response to MMP-1 and MMP-2. Biomaterials. 2010; 31(30):7836–7845. [PubMed: 20667588]
19. Zhu J. Bioactive modification of poly(ethylene glycol) hydrogels for tissue engineering. Biomaterials. 2010; 31(17):4639–56. [PubMed: 20303169]
20. Anseth KS, et al. In situ forming degradable networks and their application in tissue engineering and drug delivery. J Control Release. 2002; 78(1–3):199–209. [PubMed: 11772461]
21. Metters AT, Anseth KS, Bowman CN. Fundamental studies of a novel, biodegradable PEG-b-PLA hydrogel. Polymer. 2000; 41(11):3993–4004.
22. West JL, Hubbell JA. Polymeric Biomaterials with Degradation Sites for Proteases Involved in Cell Migration. Macromolecules. 1998; 32(1):241–244.

23. Miller JS, et al. Bioactive hydrogels made from step-growth derived PEG–peptide macromers. Biomaterials. 2010; 31(13):3736–3743. [PubMed: 20138664]
24. Xue L, et al. The Cysteine-Free Fibroblast Growth Factor 1 Mutant Induces Heparin-Independent Proliferation of Endothelial Cells and Smooth Muscle Cells. Journal of Surgical Research. 2000; 92(2):255–260. [PubMed: 10896831]
25. Mellin TN, et al. Acidic Fibroblast Growth Factor Accelerates Dermal Wound Healing in Diabetic Mice. Journal of Investigative Dermatology. 1995; 104(5):850–855. [PubMed: 7537778]
26. Singer AJ, CAF. Cutaneous Wound Healing. The New England Journal of Medicine. 1999; 341(10):738–746. [PubMed: 10471461]
27. Lee SH, et al. Poly(ethylene glycol) hydrogels conjugated with a collagenase-sensitive fluorogenic substrate to visualize collagenase activity during three-dimensional cell migration. Biomaterials. 2007; 28(20):3163–3170. [PubMed: 17395258]
28. Moon JJ, et al. Biomimetic hydrogels with pro-angiogenic properties. Biomaterials. 31(14):3840–7. [PubMed: 20185173]
29. Bryant SJ, et al. Crosslinking Density Influences Chondrocyte Metabolism in Dynamically Loaded Photocrosslinked Poly(ethylene glycol) Hydrogels. Annals of Biomedical Engineering. 2004; 32(3):407–417. [PubMed: 15095815]
30. DeKosky BJ, et al. Hierarchically Designed Agarose and Poly(Ethylene Glycol) Interpenetrating Network Hydrogels for Cartilage Tissue Engineering. Tissue Engineering Part C: Methods. 2010; 16(6):1533–1542. [PubMed: 20626274]
31. Shireman PK, et al. The S130K fibroblast growth factor-1 mutant induces heparin-independent proliferation and is resistant to thrombin degradation in fibrin glue*1. Journal of Vascular Surgery. 2000; 31(2):382–390. [PubMed: 10664506]
32. Turturro MV, PG. Generation of Mechanical and Biofunctional Gradients in PEG Diacrylate Hydrogels by Perfusion-Based Frontal Photopolymerization. J Biomater Sci Polym Ed. 2011 Apr 4. [Epub ahead of print].
33. Solon J, et al. Fibroblast adaptation and stiffness matching to soft elastic substrates. Biophys J. 2007; 93(12):4453–61. [PubMed: 18045965]
34. Levental I, Georges PC, Janmey PA. Soft biological materials and their impact on cell function. Soft Matter. 2007; 3(3):299–306.
35. Nemir S, West JL. Synthetic materials in the study of cell response to substrate rigidity. Ann Biomed Eng. 38(1):2–20. [PubMed: 19816774]

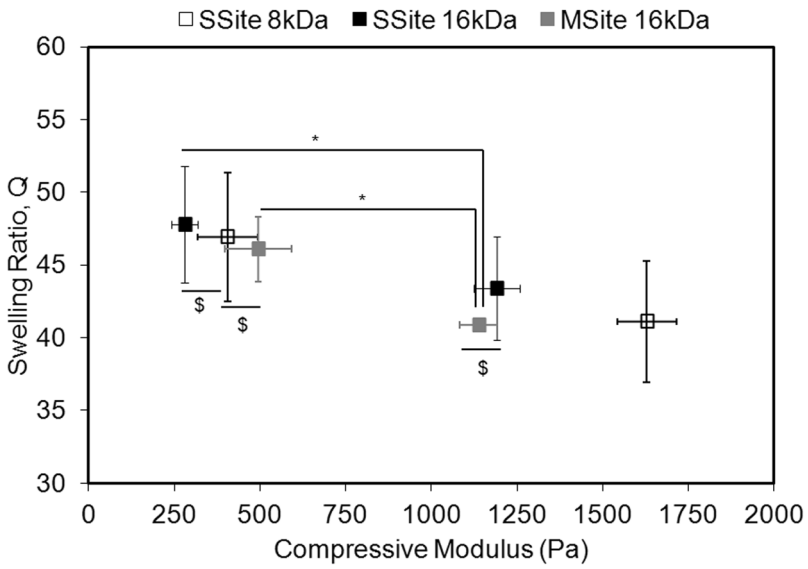

Fig. 1.

Mechanical and physical characterization of SSite and MSite PEG hydrogels. Swelling ratio as a function of compressive modulus. Data represent mean ±S.D. (n=4). Compressive modulus values statistically different with $P<0.05$ unless denoted with $, $= statistically not different. * indicates statistical significance among swelling ratios with $P<0.05$.

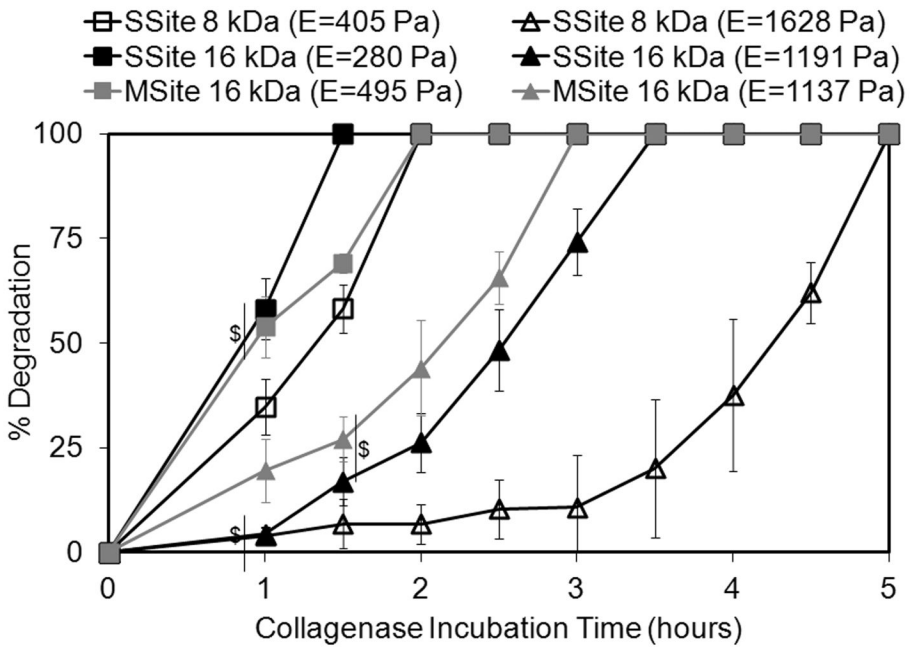

Fig. 2.

Degradation profiles of SSite and MSite collagenase-sensitive PEG hydrogels of varying compressive modulus in collagenase enzyme solution. Data represent mean ± S.D. (n=3). Degradation values are statistically different at each time point with $P<0.05$ unless denoted with $, $= statistically not different.

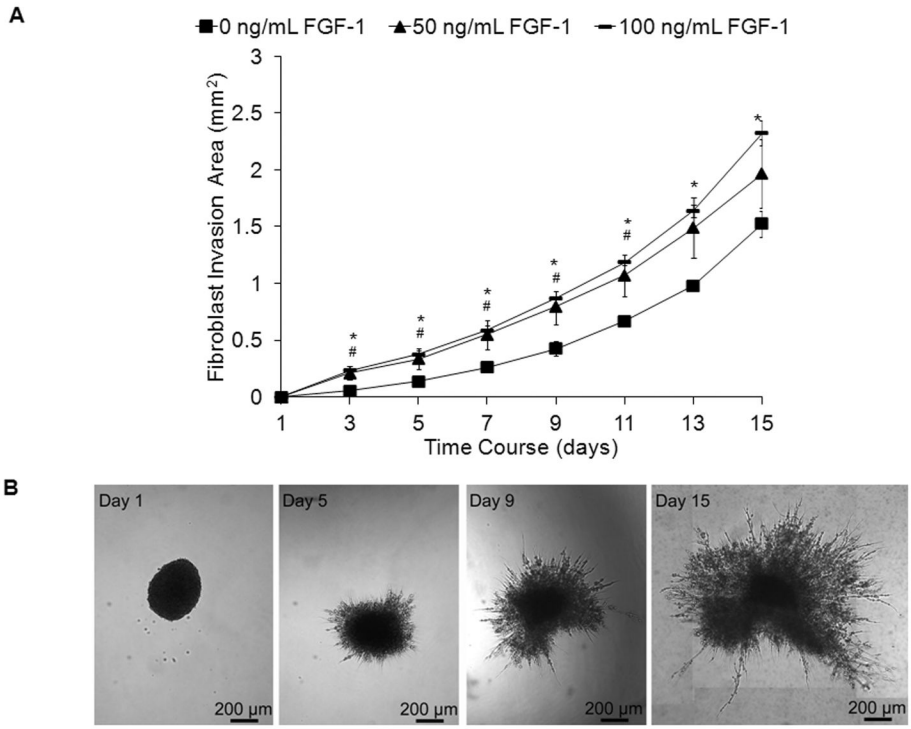

Fig. 3.

(A). Time course of fibroblast invasion within MSite PEGDA hydrogels with 0, 50, and 100 ng/mL FGF-1 and 5 U/mL heparin. Data represent mean ±S.D. (n=4). #,* indicate statistical significance of 50 and 100 ng/mL FGF-1 groups compared to 0 ng/mL FGF-1 control, respectively ($P<0.05$). (B). Corresponding images of invading fibroblast aggregates in MSite gels without the addition of FGF-1.

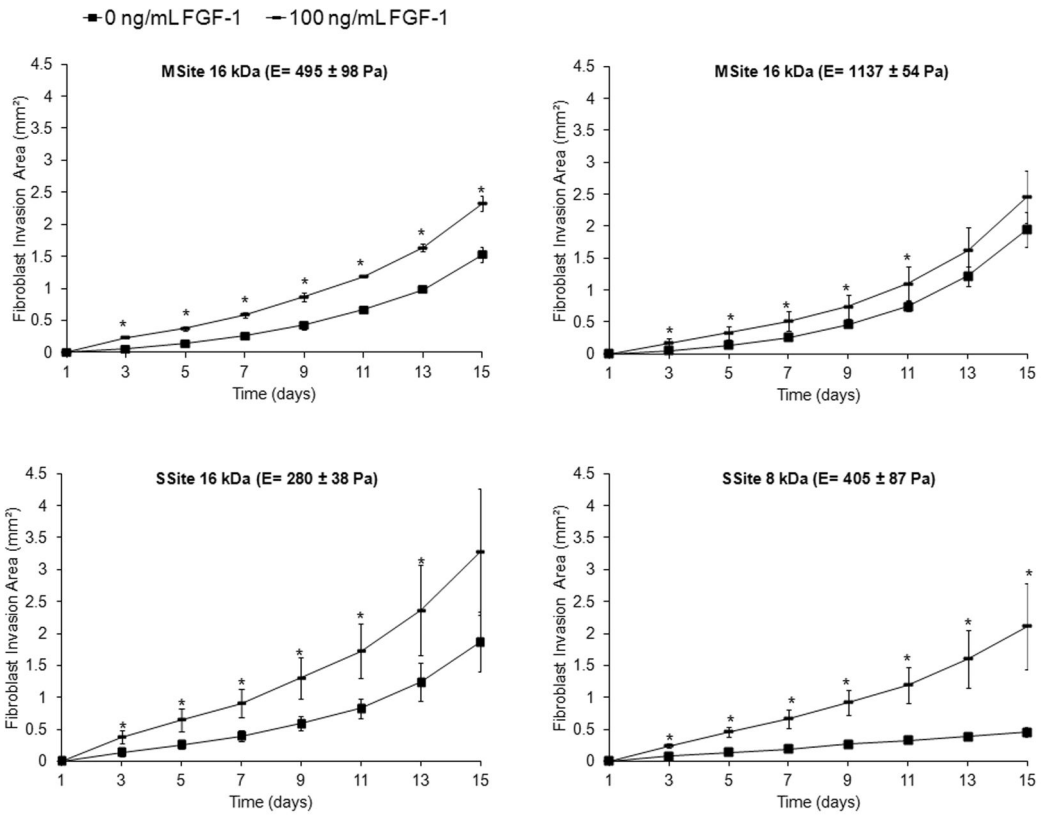

Fig. 4.

Time course of fibroblast invasion comparing all PEG hydrogel types with 0 and 100 ng/mL FGF-1 and 5 U/mL heparin. Data represent mean ±S.D. (n=4).* indicates statistical significance of 100 ng/mL FGF-1 group compared to no FGF-1 control ($P<0.05$).

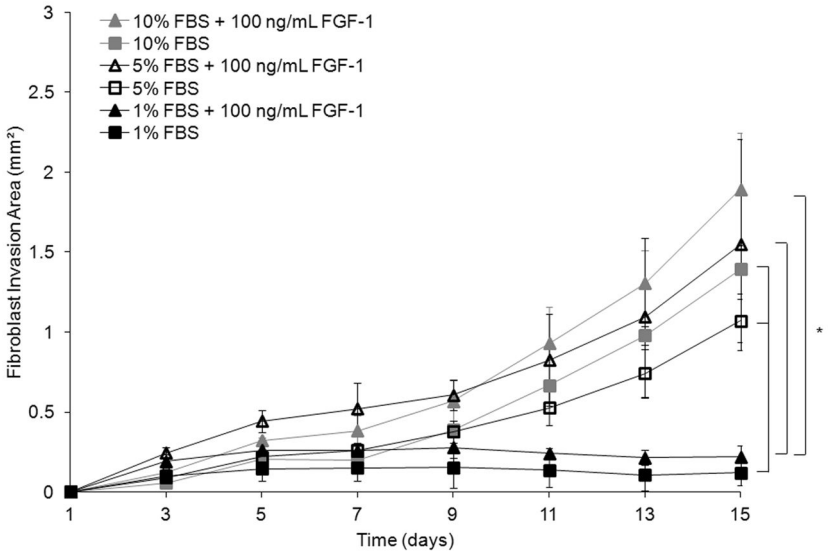

Fig. 5.

Time course of fibroblast invasion in MSite PEGDA hydrogels as a function of serum concentration (%) with 0 and 100 ng/mL FGF-1 and 5 U/mL heparin. Data represent mean ±S.D. ($n \geq 3$) ($P < 0.05$).

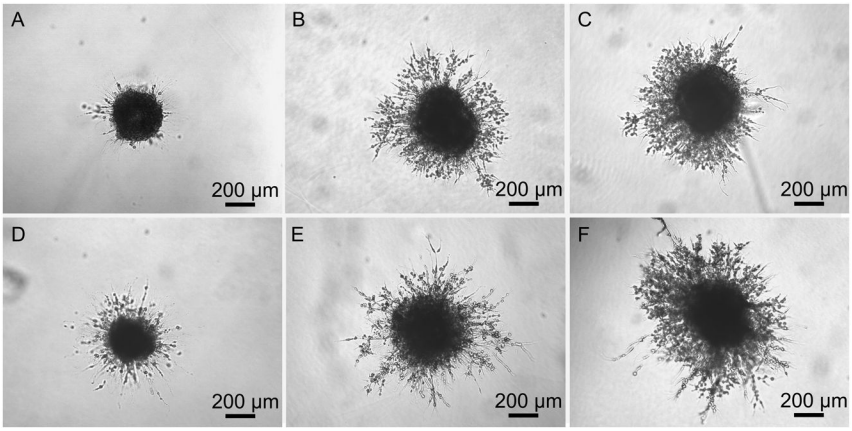

Fig. 6.

Phase contrast images of fibroblast invasion in MSite PEGDA hydrogels with 0 (A–C), and 100 ng/mL (D–F) soluble FGF-1 as a function of serum concentration with 1% serum (A, D), 5% serum (B, E), and 10% serum (C, F) on day 9.

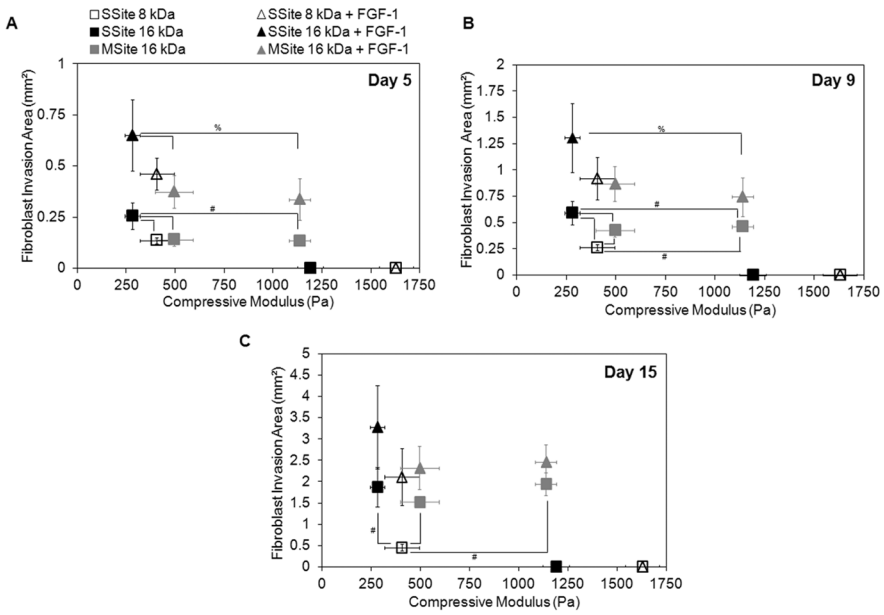

Fig. 7.

(A–C). Fibroblast invasion on days 5, 9, and 15 with 0 and 100 ng/mL FGF-1 and 5 U/mL heparin comparing the range of compressive modulus values among all PEG hydrogel types that support invasion. A decrease in the compressive modulus and the addition of FGF-1 results in an increase in fibroblast invasion. MSite hydrogels support invasion over a wider range of compressive modulus values compared to SSite hydrogels. Data represent mean ±S.D. (n=4). #,% indicate statistical significance among varying PEG types within the no FGF-1 control group and the 100 ng/mL FGF-1 group, respectively ($P<0.05$).

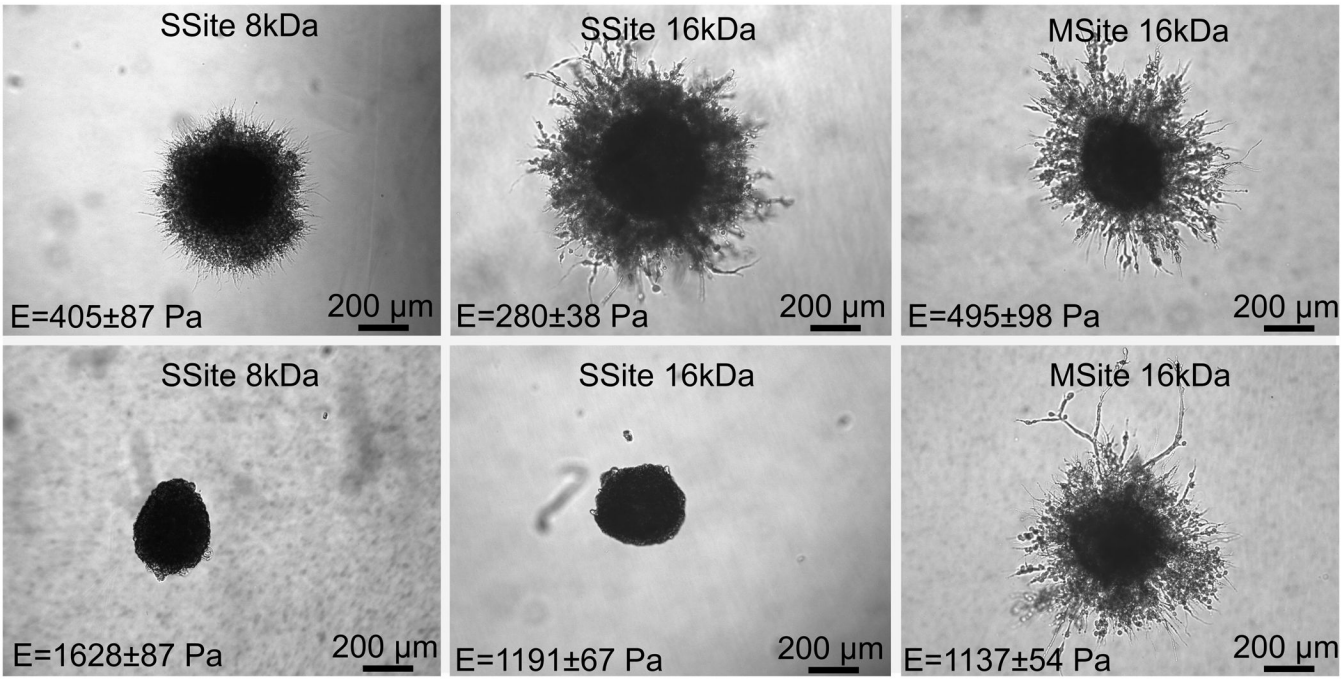

Fig. 8.

Phase contrast images of fibroblast invasion within PEG hydrogels without the addition of FGF-1 as a function of compressive modulus and varying PEG type on day 9. MSite hydrogels support invasion at both compressive modulus conditions investigated, which is not observable in SSite hydrogels.

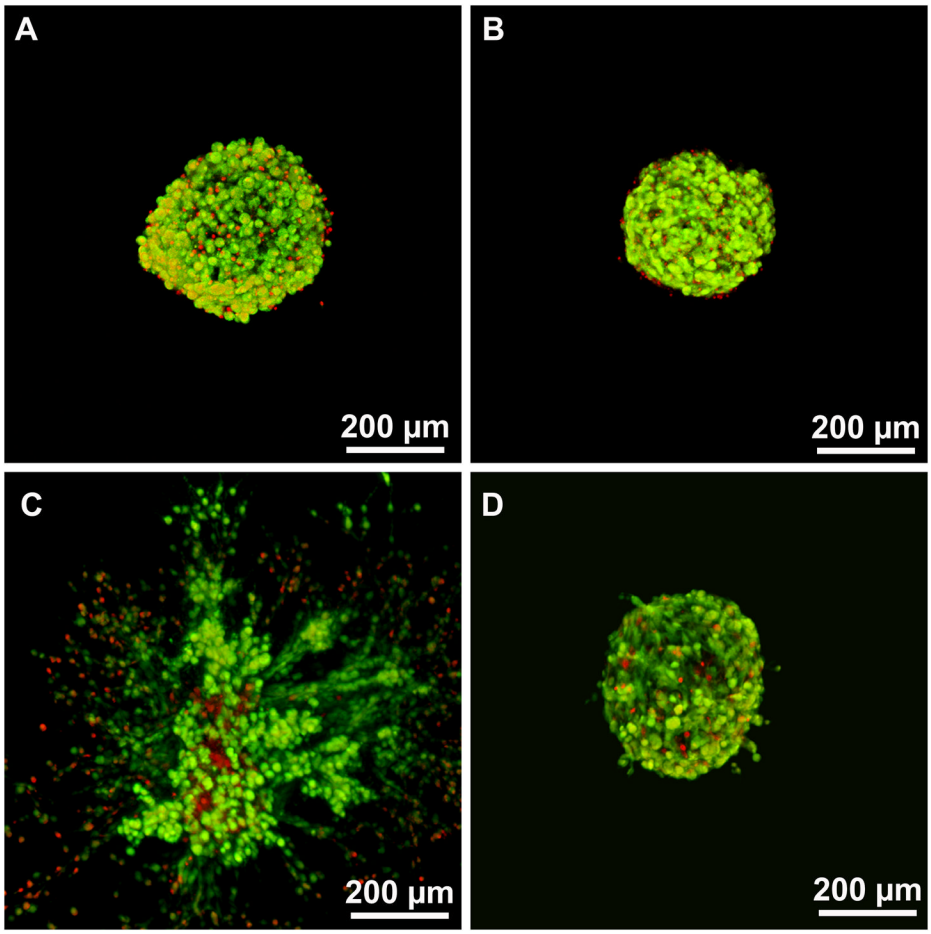

Fig. 9.

Confocal images of fibroblast aggregate LIVE/DEAD staining in SSite 16kDa PEG hydrogels 24 hrs (A,B) and 15 days (C,D) post encapsulation in: (A,C) hydrogels with compressive modulus of 280±38 Pa which supported invasion after 15 days and (B,D) hydrogels with modulus value of 1191±67 Pa which did not support invasion. Live cells are stained green and dead cells are stained red.

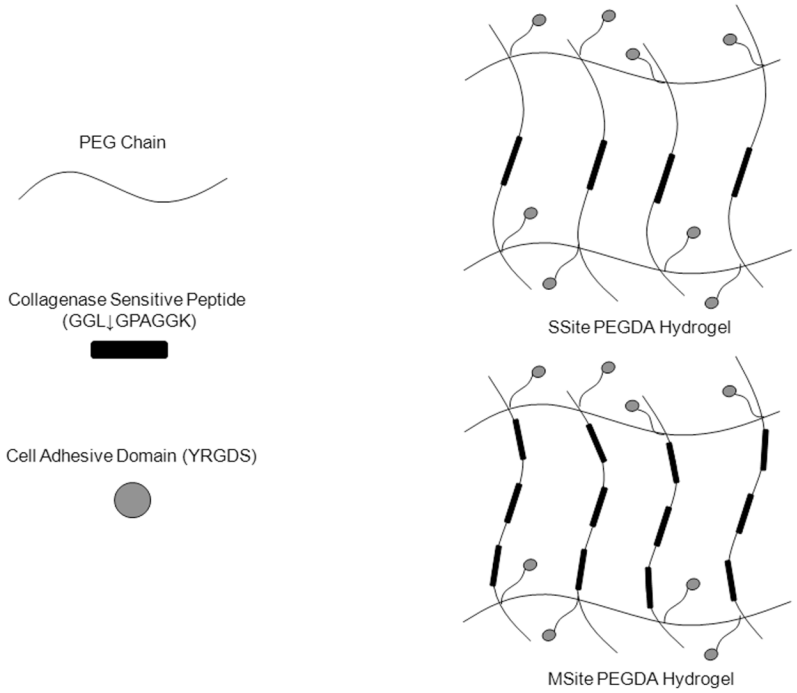

Scheme 1.

Schematic representation of SSite and MSite PEGDA macromers and the resultant hydrogel structures containing single (SSite) and multiple (MSite) collagenase-sensitive domains within crosslinks. ↓ indicates the degradation site by collagenase.